Microcrystalline Cellulose From Oil Palm Empty Fruit Bunches as Filler in Polylactic Acid

M.K. Mohamad Haafiz[1*], Azman Hassan[2*], Reza Arjmandi[2], Zainoha Zakaria[3], M.M. Marliana[2], Muhammad I. Syakir[1] and M.R. Nurul Fazita[1]

[1]School of Industrial Technology, Universiti Sains Malaysia, Penang 11800, Malaysia

[2]Department of Bioprocess and Polymer Engineering, Faculty of Chemical and Energy Engineering, Universiti Teknologi Malaysia, Skudai, Johor Bahru 81310, Malaysia

[3]Faculty of Science, Universiti Teknologi Malaysia, Skudai, Johor Bahru 81310, Malaysia

SUMMARY

Acid hydrolysis method was used to isolate microcrystalline cellulose (MCC) from oil palm empty fruit bunches (OPEFB) total chlorine free bleached pulp. The derived MCC was incorporated into polylactic acid (PLA) using solution casting technique in order to produce PLA/MCC composites. The chemical structure of the cellulose fragments remains unaltered as demonstrated by Fourier transform infrared spectroscopy despite acid hydrolysis. X-ray diffraction showed that the MCC has a cellulose I polymorph with 87% crystallinity index. The addition of MCC into PLA enhanced not only the thermal stability but also the Young's modulus of the PLA/MCC composites by approximately 30% at 5 phr MCC contents compared to pure PLA. However a decrease in tensile strength and elongation at break of the PLA/MCC composites were observed due to the poor dispersion of MCC in the PLA matrix

Keywords: Microcrystalline cellulose; Oil palm empty fruit bunch; Polylactic acid; Tensile properties; Thermal properties

1. INTRODUCTION

Global consumption of biodegradable polymers has demonstrated strong growth over the last few years due to environmental concerns such as solid waste disposal problems and the shortage of petroleum resources[1]. Polylactic acid (PLA) is a biodegradable, biocompatible and compostable polymer derived from annually renewable sources such as corn and potato and is easily processed on standard plastics equipment to yield molded parts, film or fibers for use in industrial packaging and medical devices[2,3].

Despite is desired physical characteristics such as high strength and biocompatibilities, PLA has several disadvantages such as low thermal stability and brittle nature which limit its use in certain applications particularly in the film extrusion industry[4,5]. Essentially, reinforcing filler is of importance to properties improvement as blending is much more cost-effective than copolymerization. Moreover, it is a convenient method for preparing materials with improved properties[5]. In fact, the use of reinforcing fillers such as nanoclays in polymeric materials to improve its properties has been widely reported[6]. However, substituting nanoclay with cellulose based reinforcement is a better alternative for a fully degradable and renewable nanocomposite production[7].

Microcrystalline cellulose (MCC) is potential cellulosic filler for polymers. It is basically crystalline cellulose derived from high quality wood pulp and expected to disintegrate into cellulose whisker after complete hydrolysis[8]. Due to its biodegradable material, MCC has been widely used in different industrial fields such as pharmaceuticals, cosmetics, medical applications, food processing and structural composites[9,10]. Besides that, MCC has the added advantage of high specific surface area compared to other conventional cellulose fibers[8]. The use of MCC as novel green filler in the polymer matrices to develop environmental friendly composites has been widely reported[9-12]. Chuayjuljit *et al.*[13] reported an increase in tensile strength and Young's modulus when MCC is used as reinforcement in polyvinyl chloride. Mathew *et al.*[8] produced PLA/MCC composites by using twin-screw extrusion process in an effort to disperse MCC in the PLA

*Corresponding authors: azmanh@cheme.utm.my; mhaafiz@usm.my

matrix during the extrusion process. The authors observed an improvement in the storage modulus of PLA/MCC composites with the addition of MCC.

In the present study, PLA based biodegradable composites were prepared using MCC as fillers through solution casting method. MCC was isolated from oil palm empty fruit bunches (OPEFB) total chlorine free (TCF) bleached pulp. Given that Malaysia has abundant supply of oil palm fibrous material generated by the palm oil industry and are readily available at minimal cost. Therefore is of great interest to develop a technique which can process these bio-residuals into high-value products (i.e., MCC)[14]. The crystallinity of the MCC was analyzed using X-ray diffraction (XRD). The effect of MCC loading on the thermal stability of PLA/MCC composites was investigated using thermogravimetric analysis (TGA). Subsequently, the tensile properties of the resulting PLA/MCC composites with different MCC contents were examined followed by the analysis of the composites fracture surfaces morphology using field emission scanning electron microscopy (FESEM).

2. MATERIALS AND METHOD

2.1 Materials

Sabutek (Malaysia) is a supplier for fibrous strand of OPEFB, the raw materials for MCC isolation. TCF pulping and bleaching of OPEFB-pulp prior to MCC production was performed as reported earlier by Leh *et al.*[15]. Ammonium hydroxide (NH_4OH) and 32% hydrochloric acid (HCl) were used for extracting MCC (purchased from Merck, Malaysia). The commercial MCC with a particle size of ~50 μm (Avicel® PH-101) provided by Sigma Aldrich was used as reference and denoted as C-MCC. PLA (3001D) was provided by NatureWork® LLC, Minnetonka MN, USA, in pellet form and used as polymer matrix. Its density is 1.24 g/cm^3 and melt flow index (MFI) is about 15 g/10 min (190 °C/2.16 kg). Chloroform is used as reagent, provided by Merck, Malaysia.

2.2 Preparation of Microcrystalline Cellulose

The MCC was isolated from OPEFB-pulp as reported by Chuayjuljit *et al.*[13]. The isolation was based on original procedures described by Battista[16]. The OPEFB-pulp was hydrolyzed with 2.5N HCl at 105 °C ± 2 °C for 30 minutes with 1:20 ratio (pulp:liquor). 5% diluted NH_4OH was used to wash the reaction mixture. The process was performed repetitively with distilled water in order to ensure that the mixture is acid free. Subsequently, the MCC derived from OPEFB-pulp was filtered at room temperature and then dried in a vacuum oven at 105 °C until a constant weight is achieved. The MCC was ground to fine powder using a rotary ball mill. The final form of MCC is a fine snowy-white powder[10].

2.3 Preparation of PLA and PLA/MCC Composites Film

PLA solution was prepared by stirring the PLA pellets (10 g) in 64 ml chloroform at 60 °C for 2 hours using a water bath until the pellets were fully dissolved[17]. The dissolved PLA was immediately casted using a caster knife on the clean glass plates and left for 48 hours at ambient temperature to allow the solvent evaporation[7]. The thickness of the casted PLA film was approximately 100 μm and designated as PLA.

For the PLA/MCC composites fabrication, 10 g of PLA was mixed with 64 ml chloroform and different MCC loading [1, 3 and 5 part per hundred resin (phr)]. The mixture was kept at 60 °C using a water bath with strong agitation until the PLA pellets were fully dissolved[7]. The suspension was then sonicated for 5 minutes and immediately casted on clean glass plates to produce composites with 100 μm thickness. The resultant composites were designated as PLA/MCC1, PLA/MCC3 and PLA/MCC5.

3. CHARACTERIZATION

3.1 Fourier Transform Infrared Spectroscopy

Fourier transform infrared (FT-IR) analysis was performed by using Perkin Elmer 1600 Infrared Spectrometer through pressed-disk technique. It was recorded by Nicolet's AVATAR Model 360 at 32 scans within the wave number range of 4000 to 400 cm^{-1}. The significant transmittance peak at a particular wave number was measured using the "find peak tool" provided by Nicolet OMNIC 5.01 software.

3.2 X-ray Diffractions Analysis

SIEMENS Diffractometer D5000 was used to study the crystallinity of the composite samples. X-ray diffraction (XRD) patterns were recorded using Cu Kα radiation at 40 kV and 50 mA. The samples were exposed at an angular incidence of 10° to 60° (2θ angle range). The crystallinity of the samples were calculated from diffraction intensity data using the empirical method for native cellulose and were determined using Equation (1)[7,18].

$$C_r.I(\%) = \frac{I_{002} - I_{am}}{I_{002}} \quad (1)$$

where $C_r \cdot I$ is the crystallinity index, I_{002} is the maximum intensity (in arbitrary units) of the diffraction from the 002 plane at 2θ = 22.6°, and I_{am} is the intensity of the background scatter measured at 2θ =19°.

3.3 Thermogravimetric Analysis

The thermal stability of the pure PLA and PLA/MCC composites were characterized using a thermal gravimetric analyzer model 2050, (TA Instruments, New Castle, DE). The heating rate was set at 10 °C/min over

a temperature range of 30 °C to 600 °C and measurements were carried out in nitrogen atmosphere.

3.4 Tensile Testing

The tensile property of the pure PLA and PLA/MCC composites were determined according to ASTM D882-12. The tensile test was carried out on an Instron 4400 universal testing machine with a crosshead speed of 12.5 mm/min at room temperature. Five samples were tested and the results were presented as an average for tested samples.

3.5 Field Emission Scanning Electron Microscopy

The morphology of the fractured PLA and PLA/MCC composites were analyzed using FESEM model Leo Supra, 50 VP, Carl Ziess, SMT, Germany with accelerating voltage of 10kV. The samples were mounted on an aluminum stub and were sputter-coated with gold to avoid charging.

4. RESULTS AND DISCUSSIONS

4.1 FT-IR Analysis

The OPEFB-pulp, MCC and C-MCC were characterized by FT-IR and their absorbance spectra are illustrated in **Figure 1**. FT-IR spectroscopy demonstrated the similarities between all spectra indicating that all the samples have the same functional groups. The broad absorption band located at 3400-3500 cm^{-1} is attributed to the stretching of -OH groups[18]. This band was found to be broader in range for OPEFB-pulp spectrum (**Figure 1a**) compared to the others. This is due to the greater number of OH groups present in the glucose units of cellulose pulp chain polymers compared to MCC chain polymers[19]. The absorption peak at 1645 cm^{-1} in all samples implies the presence of –OH in cellulose where this peak is related to the bending mode of water molecules due to strong interaction between cellulose and water[7,18,20]. The absorption band at 1425 cm^{-1} observed in all samples is associated with intermolecular hydrogen at the C_6 group[7,21]. A medium absorption peak at 2900 cm^{-1} is related to CH_2 groups[18]. The absorption band at 1163 cm^{-1} is assigned to the C–O–C stretching, and the peak at 896 cm^{-1} is associated with C-H rock vibration of cellulose (anomeric vibration, specific for β-glucosides)[7].

According to previous works, researchers had claimed that the absence of peaks located in the range 1509-1609 cm^{-1} which corresponds to C=C aromatic skeletal vibrations, demonstrated the complete removal of lignin[18,22]. The absorption band which corresponds to either acetyl or uronic ester groups of hemicelluloses normally appear in the range 1700-1740 cm^{-1}, while its absence indicates the successful removal of hemicelluloses during pulping and bleaching process[7]. This is in agreement with Jahan *et al.*[25] for the production of MCC from jute fibers. The FT-IR spectra showed that the chemical structure of cellulose fragments stay unaltered despite the hydrolysis process on OPEFB-pulp.

According to previous works, researchers had claimed that the absence of peaks located in the range 1509-1609 cm^{-1} which corresponds to C=C aromatic skeletal vibrations, demonstrated the complete removal of lignin[18,22]. The absorption band which corresponds to either acetyl or uronic ester groups of hemicelluloses normally appear in the range 1700-1740 cm^{-1}, while its absence indicates the successful removal of hemicelluloses during pulping and bleaching process[7]. This is in agreement with Jahan *et al.*[25] for the production of MCC from jute fibers. The FT-IR spectra showed that the chemical structure of cellulose fragments stay unaltered despite the hydrolysis process on OPEFB-pulp.

4.2 X-Ray Diffraction Analysis

The XRD patterns of OPEFB-pulp, MCC and C-MCC were shown in **Figure 2a-c**, respectively. **Figure 2** shows the highly crystalline native cellulose I with non-existing cellulose II for all samples, indicated by the absence of a doublet located at 22.6°[18]. The crystallinity values

Figure 1. FT-IR spectra obtained of (a) OPEFB-Pulp, (b) MCC and (c) C-MCC

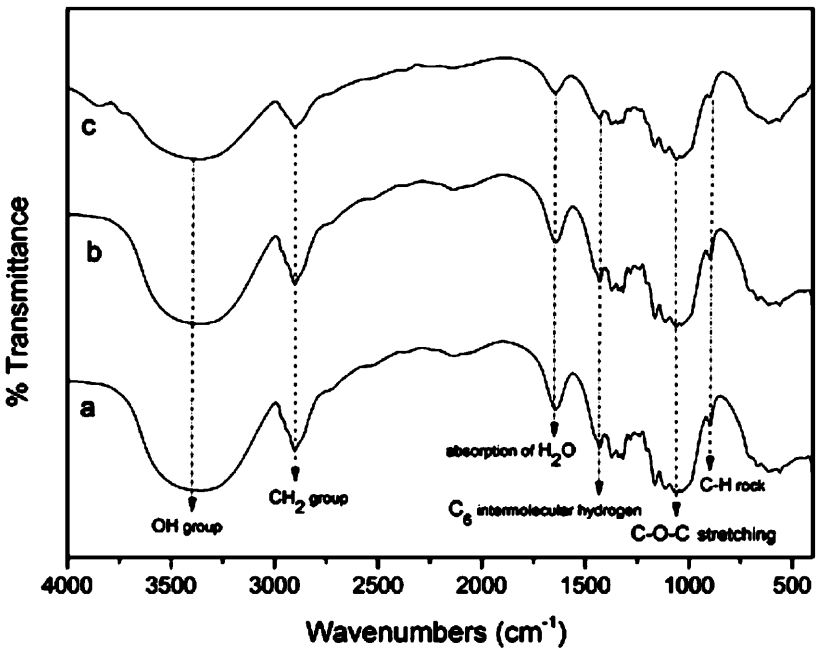

Figure 2. X-Ray diffraction of (a) OPEFB-Pulp, (b) MCC and (c) C-MCC

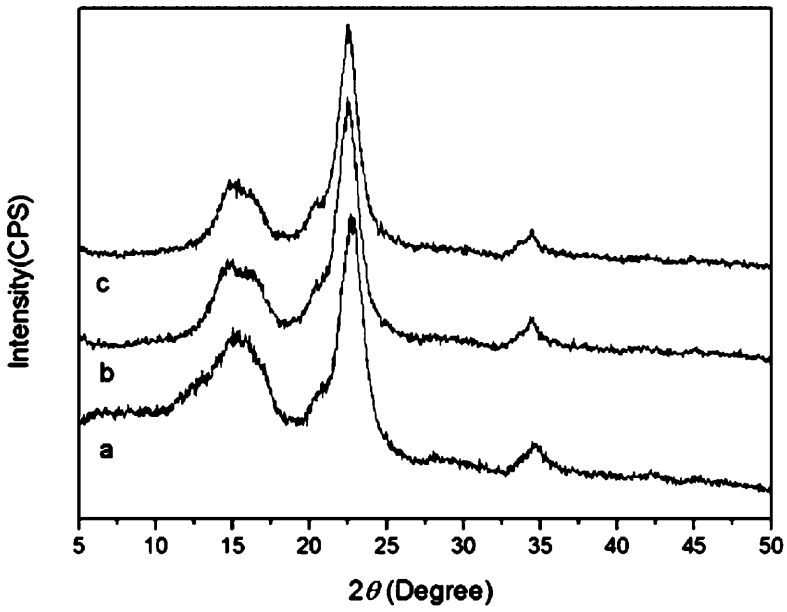

of OPEFB-pulp, MCC and C-MCC are summarized in **Table 1**. The crystallinity index for MCC is higher than OPEFB-pulp, due to the removal of the amorphous regions of cellulose by acid hydrolysis. This prompts the hydrolytic cleavage of glycosidic bonds to release individual crystallites[23]. High crystallinity index is related to an increase in rigidity of the cellulose structure, which can lead to higher tensile strength for fibers, hence, it is expected to enhance the mechanical performance of composites[7,18,24]. In this study, the obtained MCC from OPEFB-pulp exhibits higher crystallinity index as compared to the MCC by Jonoobi *et al.*[3], who reported only 69% crystallinity (chemo-mechanical technique). Meanwhile, another study on the isolation of MCC from jute using H_2SO_4 was reported to have ~75% crystallinity[25].

Table 1. Crystallinity of OPEFB-Pulp and MCC as compared to C-MCC

Sample	Crystallinity %
OPEFB-Pulp	80
MCC	87
C-MCC	79

4.3 Thermogravimetric Analysis

The resultant MCC was used as fillers in the fabrication of PLA/MCC composites. The effect of MCC content on the thermal stability of PLA/MCC composites was studied using TGA. The TGA curves (weight% *vs.* temperature °C) of PLA and PLA/MCC composites with various MCC contents have shown in **Figure 3**. The onset decomposition temperature (T_{on}) as well as $T_{10\%}$ and $T_{50\%}$ decomposition temperature for all PLA/MCC composites is higher than pure PLA (T_{on}= 295.93 °C). It is evident that the thermal stability of PLA increases with the addition of MCC fillers. The shifting of $T_{on,}$ $T_{10\%}$ and $T_{50\%}$ decomposition temperatures to higher temperatures showed an improvement in the interaction between the fillers and the polymer matrix[8].

From the TGA curves (**Figure 3**), it is observed that both pure PLA and PLA/MCC composites only have one-step degradation stage that represented by single peaks. Similar result was reported by Zhou *et al.*[9], where MCC was used as reinforcement in poly(3-hydroxybutyrate-co-3-hydroxyvalerate). Interestingly, the PLA/MCC5 composite demonstrated higher char residue (2.4%) compared to pure PLA and PLA/MCC3 composite. This behavior may be due to the presence of higher amount of crystalline cellulose I from the resultant MCC which has an intrinsically flame resistant property[10]. It can be concluded that the incorporation of MCC into PLA matrix improved the thermal stability of pure PLA. This result is in agreement with Chuayjuljit *et al.*[13] who reported

Figure 3. TGA curves for pure PLA and PLA/MCC composites

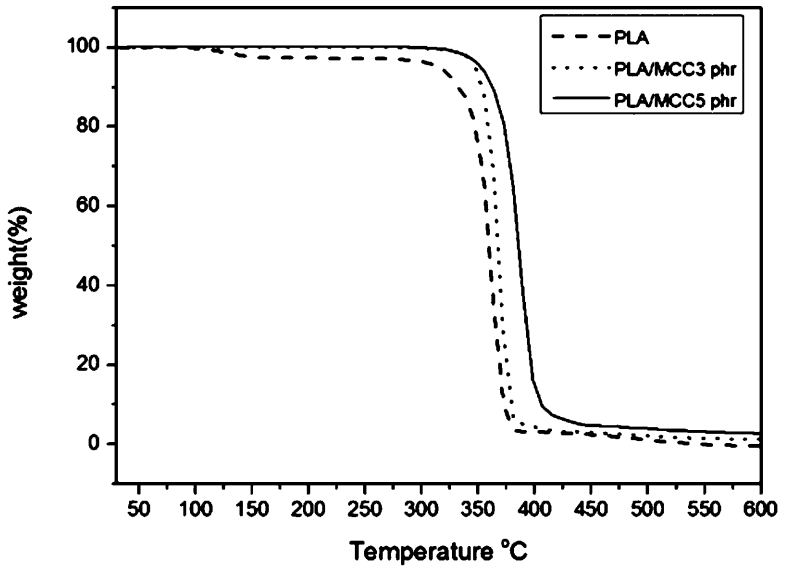

similar results on the effect of MCC filled polyvinyl chloride film where the MCC obtained prepared from cotton fabric waste.

4.4 Tensile Properties

Figure 4 shows the influence of MCC contents on the tensile strength, elongation at break and Young's modulus properties of PLA/MCC composites. Evidently, the figure illustrated that the incorporation of MCC into PLA matrix imposed negative effect on both the tensile strength and elongation at break of the PLA/MCC composites compared to pure PLA, while the PLA/MCC composite Young's modulus increased with increasing MCC content.

Figure 4a depicts a drastic decline of tensile strength in PLA with the addition of MCC fillers. This trend continues to decline inversely with MCC content. Such low tensile strength for the composites is accentuated by the probable aggregation of the MCC, leading to the formation of weak points[26]. This poor dispersion and lack of good adhesion between the fillers and the matrix may lead to the formation of numerous voids at the filler-matrix interface, resulting in low tensile strength values due to poor stress transfer from the matrix to the fillers[27]. This result is in agreement with Qu *et al.*[28] and Yew *et al.*[26].

In addition, from the observation (**Figure 4a**), elongation at break also decreased gradually with increasing MCC concentrations, suggesting that the elongations at break for all PLA/MCC composites are lower than pure PLA. This is due to the stiffening action of the filler which restricts the segmental chain movement of PLA during tensile testing[10]. According to Pei *et al.*[29], the elongation at break is affected by the volume fraction of the added reinforcements, the dispersion of the reinforcement in the matrix and the interaction between the reinforcement and the matrix. The aggregation of the MCC in the PLA matrix can be observed from the fractured surface of PLA/MCC5 composite (**Figure 5**), suggesting poor dispersion of MCC in the PLA matrix. Furthermore, poor interactions between the fillers and PLA matrix led to substantial local stress concentration and deteriorated the elongation at break of PLA/MCC composites.

Figure 4b shows that the PLA filled with 5 phr MCC fillers has higher Young's modulus (4.6 GPa) compared to pure PLA (3.9 GPa). The higher Young's modulus of the PLA/MCC5 composite compared to pure PLA can be explained by the increase in hydrogen bonding that improves the mechanism of load transfer to the fillers, stiffening effect and higher crystallinity of the composites[8,27,30]. PLA is a semicrystalline polymer and the crystallinity of PLA is predicted to increase with the addition of MCC, therefore, resulting in higher Young's modulus[27]. For the tensile performance of PLA/MCC composites, the addition of MCC has a negative impact on the tensile strength and elongation at break of the composites compared to pure PLA, which could be due to the agglomeration of MCC particles, as indicated by arrows in **Figure 5**.

Figure 4. Effect of MCC loading on tensile properties of PLA/MCC composites: (a) elongation at break (%) and tensile strength and (b) Young's modulus

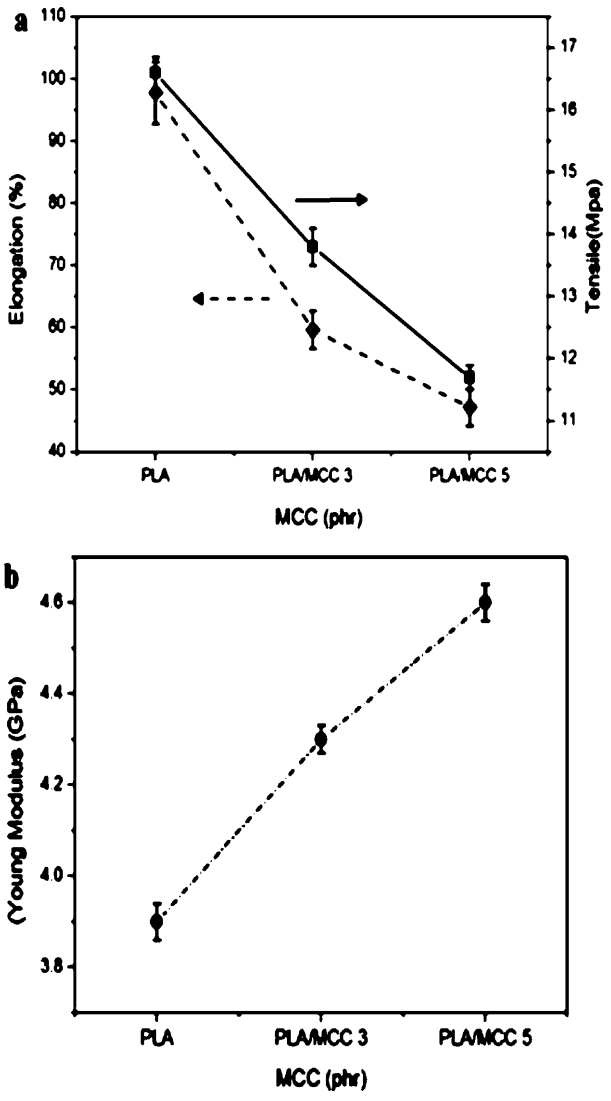

Figure 5. FESEM micrographs of fractured cross-sections of PLA/MCC5 composite

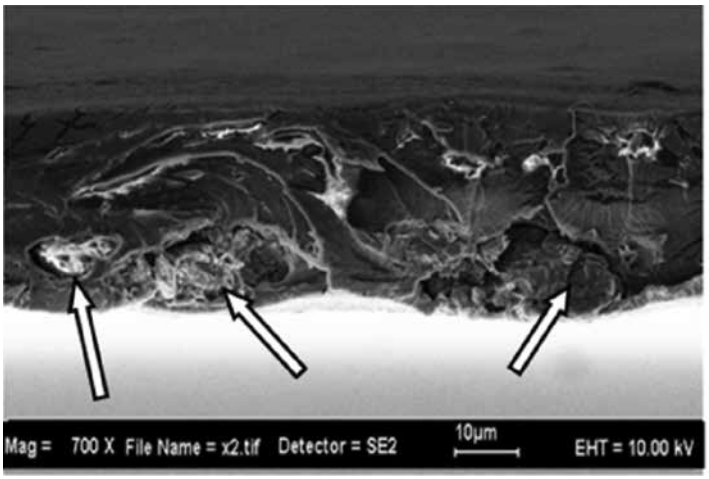

5. CONCLUSIONS

MCC has been successfully isolated from OPEFB-pulp and used as filler in the PLA matrix. The FT-IR analysis demonstrated that the acid hydrolysis did not affect the chemical structure of the cellulosic fragments. XRD study revealed that the MCC has cellulose I structure and high crystallinity index relative to OPEFB-pulp. Thermal characterization indicated that the PLA/MCC composites have better thermal stability compared to pure PLA. Moreover, the evaluation of the tensile properties of PLA/MCC composites demonstrated an improvement in the Young's modulus with increasing MCC content due to the stiffening action of the MCC filler. In contrast, the tensile strength and elongation at break of the PLA/MCC composites decreased inversely with MCC content, suggesting poor interfacial adhesion and poor dispersion of MCC fillers in the PLA matrix.

ACKNOWLEDGMENTS

The author, M.K Mohamad Haafiz, would like to thank for the financial support provided by University Sains Malaysia (USM) Short Term Research Grant 304/PTEKIND/6313194 and Ministry of Education for the Fundamental Research Grant Scheme (FRGS) 203/PTEKIND/6711500.

REFERENCES

1. Suryanegara L., Nakagaito A.N., and Yano, H, *Compos. Sci. Technol.*, **69** (2009) 1187-1192.
2. Garlotta D., *J. Polym. Environ.,* **9** (2001) 63-84.
3. Jonoobi M., Harun J., Mathew A.P., and Oksman K., *Compos. Sci. Technol.,* **97** (2010) 1742-1747.
4. Qu P., Goa Y., Wu G.F., and Zhang L.P., *BioResources,* **5** (2010) 1811-1823.
5. Ljungberg N., and Wesslen B., *Biomacromolcules*, **6** (2005) 1789-1796.
6. Oksman K., Mathew A.P., Bondeson D., and Kvien I., *Compos. Sci. Technol.,* **66** (2006) 2776-2784.
7. Haafiz M.K.M., Hassan A., Zakaria Z., Inuwa I.M., Islam M.S., and Jawaid M., *Carbohydr. Polym.,* **98** (2013) 139-145.
8. Mathew A.P., Oksman K., and Sain M., *J. Appl. Polym. Sci.,* **97** (2005) 2014-2025.
9. Zhou Z., Yu H., Zhu M., and Qin Z., *Adv. Mat. Res.,* **284-286** (2011) 1778-1781.
10. Haafiz M.K.M., Eichhorn S.J., Hassan A., and Jawaid M., *Carbohydr. Polym.,* **93** (2013) 628-634.
11. Silverio H.A., Netoa W.P.F., Dantas N.O., and Pasquinia D., *.Ind. Crop. Prod.,* **44** (2013) 427-436.
12. Pasquini D., Teixeira E.D., Da Silva Curvelo A.A.P., Belgacem M.N., and Dufresne A., *Ind. Crop. Prod.*, **32** (2010) 486-490.
13. Chuayjuljit S., Su-uthai S., and Charuchinda S., *Waste Manage. Res.,* **28** (2010) 109-117.
14. Wanrosli W.D., Haafiz M.K.M., and Azman, S., *BioResources,* **6** (2011) 1719-1740.
15. Leh C.P., Wanrosli W.D., Zainuddin Z., and Tanaka R., *Ind. Crop. Prod.,* **28** (2008) 260-267.
16. Battista O.A., *Ind. Eng. Chem.,* **42** (1950) 502-507.
17. Sanchez-Garcia M.D., and Lagaron J.M., *Cellulose*, **17** (2010) 987-1004.
18. Rosa S.M.L., Rehman N., De Miranda M.I.G., Nachtigall S.M.B., and Bica C.l.D., *Carbohydr. Polym.,* **87** (2010) 1131-1138.
19. Rosnah M.S., Astimar A.A., Wan H.W.H., and Ab Gapor M.T., *J. Oil Palm Res.*, **21** (2009) 613-620.
20. Johar N., Ahmad I., and Dufresne A., *Ind. Crop. Prod.,* **37** (2012) 93-99.
21. Kumar V., Maria De La L.R.M., and Yang D., *Int. J. Pharm.,* **235** (2002) 129-140.
22. Fahma F., Iwamoto S., Hori N., Iwata T., and Takemura A., *Cellulose,* **17** (2010) 977-985.
23. Spagnola C., Rodriguesa F.H.A., Pereira A.G.B., Fajardoa A.R., Rubiraa A.F., and Muniz E.C., *Carbohydr. Polym.,* **87** (2012) 2038-2045.
24. Alemdar A., and Sain M., *Bioresour. Technol.,* **99** (2008) 1664-1671.
25. Jahan M.S., Saeed A., He Z., and Ni Y., *Cellulose,* **18** (2011) 451-459.
26. Yew G.H., Mohd Yusof A.M., Mohd Ishak Z.A., and Ishiaku U.S., *Polym. Degrad. Stabil.,* **90** (2005) 488-500.
27. Siqueira G., Bras J., and Dufresne A., *Biomacromolecules,* **10** (2009) 425-432.
28. Qu P., Goa Y., Wu G.F., and Zhang L.P., *BioResources,* **5** (2010) 1811-1823.
29. Pei A., Qi Z., and Berglund L.A., *Compos. Sci. Technol.,* **70** (2005) 815-821.
30. Cheng Q., Wang S., and Rials T.G., *Compos. Part A,* **40** (2009) 218-224.